nature geoscience

LETTERS

PUBLISHED ONLINE: 4 APRIL 2010 | DOI: 10.1038/NGEO828

Links between eccentricity forcing and the 100,000-year glacial cycle

Lorraine E. Lisiecki

Variations in the eccentricity (100,000 yr), obliquity (41,000 yr) and precession (23,000 yr) of Earth's orbit have been linked to glacial–interglacial climate cycles. It is generally thought that the 100,000-yr glacial cycles of the past 800,000 yr are a result of orbital eccentricity[1–4]. However, the eccentricity cycle produces negligible 100-kyr power in seasonal or mean annual insolation, although it does modulate the amplitude of the precession cycle. Alternatively, it has been suggested that the recent glacial cycles are driven purely by the obliquity cycle[5–7]. Here I use statistical analyses of insolation and the climate of the past five million years to characterize the link between eccentricity and the 100,000-yr glacial cycles. Using cross-wavelet phase analysis, I show that the relative phase of eccentricity and glacial cycles has been stable since 1.2 Myr ago, supporting the hypothesis that 100,000-yr glacial cycles are paced[8–10] by eccentricity[4,11]. However, I find that the time-dependent 100,000-yr power of eccentricity has been anticorrelated with that of climate since 5 Myr ago, with strong eccentricity forcing associated with weaker power in the 100,000-yr glacial cycle. I propose that the anticorrelation arises from the strong precession forcing associated with strong eccentricity forcing, which disrupts the internal climate feedbacks that drive the 100,000-yr glacial cycle. This supports the hypothesis that internally driven climate feedbacks are the source of the 100,000-yr climate variations[12].

The defining aspect of the 100,000-yr (100-kyr) problem is (1) the lack of significant external forcing at that frequency[2]. Other aspects of the 100-kyr problem are[2] (2) the lack of 400-kyr power in late Pleistocene ice volume despite its presence in eccentricity; (3) an amplitude mismatch between 100-kyr cycles in eccentricity and climate[13], particularly during marine isotope stage (MIS) 11; (4) uncertainty about why 100-kyr power increased at the mid-Pleistocene transition (MPT) approximately 0.8 Myr ago; and (5) why glacial cycles show a small (but consistent) phase relative to eccentricity[4]. Furthermore, (6) too few 100-kyr glacial cycles occur in the late Pleistocene to distinguish between many possible causal mechanisms[5,14,15].

Glacial cycles are commonly characterized using the δ^{18}O of foraminiferal calcite[1–6], which measures global ice volume and ocean temperature. Previous studies have observed that the 100-kyr phase of late Pleistocene δ^{18}O is qualitatively consistent with eccentricity[1,3,4], but a statistical test found that the phases of glacial terminations and eccentricity are not correlated at the 5% significance level from 0.7 to 0 Myr ago[5] or 1 to 0 Myr ago[6]. As termination phases were found to correlate with obliquity forcing, these studies proposed that ~100-kyr cycles result from quantized bundles of 41-kyr obliquity cycles[5,6].

Here I present a modified version of that statistical test[5,6] applied to a different δ^{18}O record, the LR04 benthic stack[16]. To compare the phases of the climate response and eccentricty, the stack is assigned a new, untuned age model that is independent of orbital forcing assumptions and assumes, instead, that the globally averaged sedimentation rate is constant[4–6] (see Supplementary Information). As the LR04 stack averages data from 25 to 47 sites since 1.2 Myr ago, it constrains both the magnitude and age of δ^{18}O responses better than previous studies using 8–12 sites[4–6]. I analyse the stack's 100-kyr phase beginning at 1.2 Myr ago for three reasons: the stack's 100-kyr power rapidly increases at 1.2 Myr ago (Fig. 1); including more 100-kyr cycles improves the ability of the statistical test to evaluate the eccentricity pacing hypothesis; and the MPT may have begun as early as 1.2 Myr ago[7,17].

Previous studies[4–6] analysed the phase of 100-kyr cycles using the estimated ages of terminations because large, abrupt terminations are easily identified. However, it is not always clear which δ^{18}O changes should be considered terminations[5], and terminations are less indicative of 100-kyr phase before ~0.8 Myr ago when δ^{18}O responses are dominated by 41-kyr power. To address the question of whether eccentricity paces 100-kyr climate variability rather than whether it paces abrupt warming events, this study uses cross-wavelet analysis of benthic δ^{18}O and eccentricity to characterize the phase of ~100-kyr cycles (see the Methods section and Supplementary Information).

The 100-kyr phase of the untuned LR04 benthic stack relative to eccentricity varies between −36° (−10 kyr) and +35° (+10 kyr) from 1.2 to 0 Myr ago (Fig. 2). The Rayleigh statistic R (see the Methods section) is used to estimate the phase stability between δ^{18}O and eccentricity by sampling the cross-wavelet phase every 100 kyr from 1.2 to 0 Myr ago (Fig. 2b), yielding an R value of 0.94. For comparison, the critical R value to reject the null hypothesis at the 5% significance level is estimated to be 0.80 using 10,000 iterations of a random walk with 100-kyr 'saw-tooth' cycles (see the Methods section and Supplementary Information). Thus, the 100-kyr climate response is demonstrated to be phase locked to eccentricity since at least 1.2 Myr ago.

This finding does not necessarily conflict with the finding that obliquity paces terminations[5,6]. The primary reason why a statistically significant correlation with eccentricity is found in this study and not others[5,6] is the use of wavelets instead of instantaneous termination phases to characterize the 100-kyr phase (see Supplementary Information). Thus, obliquity and precession may influence the exact timing of terminations[13,18], whereas eccentricity may pace ice-sheet growth[4,11,19] (discussed below). The interactions of all three orbital cycles may cause termination phases to vary by as much as 90° (ref. 10).

Phase-locking mechanisms do not necessarily produce a correlation between the power of forcing and response because internal oscillations may synchronize with weak external forcing at a similar frequency[8–10]. However, a comparison of the 100-kyr power in δ^{18}O and eccentricity yields new and informative results. Figure 1

Department of Earth Science, University of California, Santa Barbara, California 93106, USA. e-mail: lisiecki@geol.ucsb.edu.

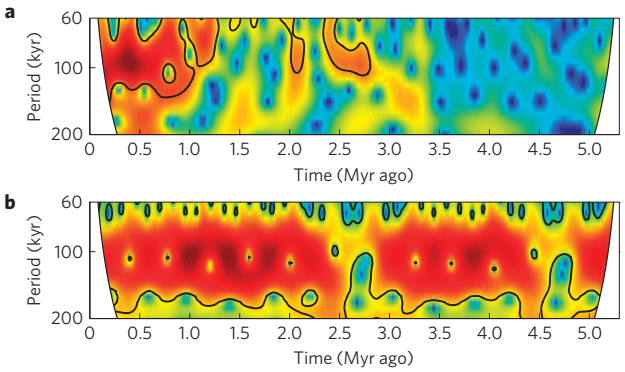

Figure 1 | Wavelet power spectra. a,**b**, Local wavelet power spectra of untuned benthic δ^{18}O (**a**) and orbital eccentricity (**b**). The black contour marks the 5% significance level against red noise.

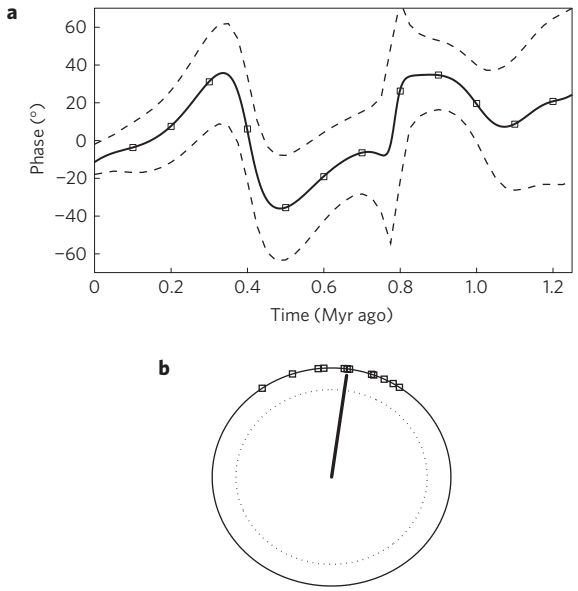

Figure 2 | 100-kyr phase. a, Phase lag of untuned δ^{18}O relative to eccentricity calculated by cross-wavelet analysis. The dashed lines are 1σ error bars based on age-model uncertainty (see Supplementary Information). The squares mark where the phase is sampled every 100 kyr for calculation of the Rayleigh statistic. **b**, Phase wheel representation of the 100-kyr phase (squares) of untuned δ^{18}O from 1.2 to 0 Myr ago. The vector length is the Rayleigh R value (0.94) and its angle shows the mean phase lag (7.7°, 1.2 kyr). The dotted circle marks the 5% significance level ($R = 0.80$) for eccentricity pacing.

shows that 100-kyr power in δ^{18}O exceeds the 5% significance level not only in the late Pleistocene but also at 2.1 Myr ago and 2.8–2.5 Myr ago and that these are all times of anomalously weak 100-kyr power in eccentricity. Figure 3 compares the 100-kyr power of δ^{18}O and eccentricity over the past 5 Myr (see the Methods section and Supplementary Information). During this time the variance of benthic δ^{18}O increases exponentially because of an increase in the sensitivity of the climate system to orbital forcing[20]. After removing this trend, the 41-kyr and 23-kyr power of δ^{18}O are positively correlated with the power of obliquity and precession forcing, respectively, throughout most of the Plio-Pleistocene[20]. In contrast, removing the exponential trend from the 100-kyr power of δ^{18}O (Fig. 3) produces a negative correlation of −0.69 between the 100-kyr power of eccentricity and detrended δ^{18}O (see the Methods section and Supplementary Information).

The exponential increase in the 100-kyr power of δ^{18}O and its anticorrelation with eccentricity power can also be described using a speculative conceptual model,

$$P_{\delta^{18}\mathrm{O}}(t') = C\mathrm{e}^{\alpha t' - \beta P_{\mathrm{ecc}}(t')} + \epsilon \quad (1)$$

where $P_{\delta^{18}\mathrm{O}}$ and P_{ecc} are power in the 100-kyr band (see the Methods section) of δ^{18}O and eccentricity, respectively, P_{ecc} is normalized to zero mean and unit variance, t' is time since 5.3 Myr ago, α and β are parameters selected to optimize the model's fit (see Supplementary Information), C is a scaling factor and ϵ is an error term. For $\alpha = 1.1$ and $\beta = 0.69$, the model explains 93% of variance in the 100-kyr power of δ^{18}O from 5 to 0 Myr ago and 89% of its increase since 1.3 Myr ago (Fig. 3a). However, if the anticorrelation with P_{ecc} is not included in the model ($\beta = 0$), the best-fit model ($\alpha = 0.9$, Fig. 3a) explains only 33% of the increase in 100-kyr response since 1.3 Myr ago (see Supplementary Information).

Although not conclusive, the good fit produced by this simple model for the entire Plio-Pleistocene suggests that the same climate dynamics may govern 100-kyr glacial cycles at least since the onset of Northern Hemisphere glaciation 2.75 Myr ago. Moreover, it suggests that the abrupt increase in 100-kyr power at the MPT may have resulted from the combined effects of a long-term exponential increase in 100-kyr power (analogous to the increase in total variance) and a decrease in the 100-kyr power of eccentricity at ~0.8 Myr ago. However, the correlation may not necessarily indicate a causal link; a mechanistic model has yet to be identified.

On the basis of these observations, I propose that eccentricity has two important roles in the 100-kyr response of Plio-Pleistocene δ^{18}O: pacing since at least 1.2 Myr ago and 'inverse' amplitude modulation (that is, anticorrelation of the 100-kyr power of eccentricity and δ^{18}O). Inverse amplitude modulation suggests that eccentricity is unlikely to force 100-kyr glacial cycles directly[21] or through a nonlinear precession response[3]. Thus, the 100-kyr response is more likely to originate from internal feedbacks of the climate system[12] that are phase locked[8–10] to eccentricity[4]. Furthermore, I propose that inverse amplitude modulation occurs because the internal climate feedbacks responsible for Plio-Pleistocene 100-kyr cycles are inhibited by strong precession forcing. The ability of strong precession forcing to disrupt the formation of 100-kyr cycles is also supported by the fact that the strongest 100-kyr cycle (MIS 11) occurs during weak precession forcing[2] and the relatively weak MIS 7 cycle occurs during strong precession forcing[13] (Supplementary Fig. S4).

Previous studies proposed that one weak precession cycle is necessary to provide enough time to grow large, unstable ice sheets that collapse the next time insolation increases above a certain threshold[4,11,13,19]. However, ice volume is probably sensitive to the cumulative effects of precession forcing over an entire eccentricity cycle[13,19]. Strong 100-kyr eccentricity cycles produce strong precession forcing over more than half of the cycle; therefore, these cycles have only 30–40 kyr of weak precession forcing (Supplementary Fig. S4) during which slow feedbacks can drive ice-sheet growth. In contrast, when the 100-kyr power of eccentricity is weak, precession forcing is weak or moderate over the entire 100-kyr cycle, and slow feedbacks have more time to generate large 100-kyr responses. It is beyond the scope of this study to determine which component of the climate system produces the 100-kyr response, but it is likely to be one with a long time constant, such as the carbon cycle or ice sheets.

The hypothesis that 100-kyr glacial cycles result from an internally driven climate oscillation phase locked to eccentricity but inhibited by strong precession forcing has the potential to resolve all six aspects of the 100-kyr problem from a mathematical perspective (as described below). However, it remains uncertain which physical mechanisms produce the slow feedbacks and sensitivity to eccentricity-driven precession modulation.

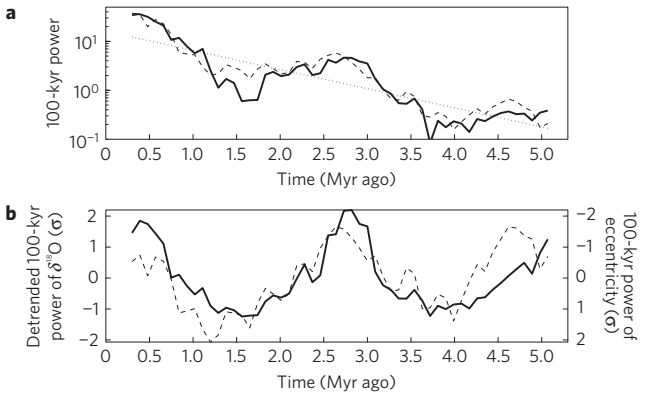

Figure 3 | Modulations in the 100-kyr power of δ^{18}O and eccentricity. (See the Methods section.) **a**, Power in the 91–129-kyr band of untuned δ^{18}O (solid line), the best-fit exponential trend for 100-kyr δ^{18}O power ($e^{0.93t'}$; dotted line) and the best-fit model of 100-kyr power (equation (1); dashed line). Note the logarithmic *y* axis. **b**, Normalized (mean = 0, standard deviation = 1) 100-kyr power of untuned δ^{18}O detrended by $e^{0.93t'}$ (solid line) and 100-kyr eccentricity power (dashed line). Note that the *y* axis for eccentricity power is flipped vertically. Furthermore, detrending has enhanced the 100-kyr power of δ^{18}O from 5 to 4.5 Myr ago; it is not statistically significant.

(1) The lack of substantial 100-kyr external forcing is not a problem if the 100-kyr response is driven primarily by internal feedbacks[8–10,12]. Terminations are triggered by precession and obliquity after large ice sheets develop[4–6,10,11,13,18,19], as paced by eccentricity (precession amplitude).
(2) A climate response phase locked to eccentricity can produce ~100-kyr cycles without generating a response to the 400-kyr eccentricity cycle[10,11].
(3) The 100-kyr power mismatch at MIS 11 is part of the overall anticorrelation between eccentricity and δ^{18}O over the past 5 Myr, which I propose occurs because strong precession forcing disrupts the internal climate feedbacks that drive 100-kyr cycles.
(4) Statistically, the MPT may result from the combined effects of an exponential trend in 100-kyr power over the past 5 Myr and a decrease in the 100-kyr power of eccentricity (and hence mean precession forcing) at ~0.8 Myr ago. However, a causal link remains to be proven.
(5) Phase-locking mechanisms can produce small phase lags[10], consistent with the estimated mean lag of 7.7° (2.1 kyr) between δ^{18}O and eccentricity since 1.2 Myr ago.
(6) The occurrence of 100-kyr glacial cycles before 0.8 Myr ago[7,17] is supported by statistically significant 100-kyr power and by a stable phase relative to eccentricity from 1.2 to 0 Myr ago. Analysing the evolution of 100-kyr responses before 0.8 Myr ago may be critical for distinguishing between different causal mechanisms[6].

An important unanswered question is how precession modulation could suppress 100-kyr glacial cycles during the early Pleistocene '41-kyr world' when the 23-kyr power of δ^{18}O is negligible. One hypothesis is that Northern Hemisphere ice volume responded to precession but that the response is largely masked in the global δ^{18}O signal because of an antiphased precession response in Antarctic ice volume[22]. Alternatively, the 100-kyr cycle may originate from processes in the tropics[7,23] or carbon cycle[12,14,24,25] that are not recorded by early Pleistocene benthic δ^{18}O. The link between eccentricity and 100-kyr glacial cycles could be further tested with new climate records that better constrain precession and carbon-cycle responses during the 41-kyr world and by improving the age model and signal-to-noise ratio of benthic δ^{18}O.

Methods

All analyses and conclusions in this manuscript apply specifically to benthic δ^{18}O. There may be differences in the phase and amplitude of δ^{18}O versus ice volume, but the magnitude of these differences cannot be evaluated at this time.

The radiometrically dated Brunhes/Matuyama and Matuyama/Gauss magnetic reversals provide age control points for the untuned stack at 0.78 and 2.6 Myr ago[26,27], respectively, and the ends of the stack are fixed at 0 and 5.325 Myr ago[16]. The remaining ages for the untuned age model are estimated by assuming a constant sedimentation rate (after compaction correction) between these four control points for each of the 57 benthic δ^{18}O records in the stack. Untuned ages are calculated for tie points spaced every 26 kyr. The Supplementary Information provides more details about this procedure and estimates of age-model uncertainty. Before spectral analysis, the untuned stack is linearly interpolated to an even 1-kyr time step (Supplementary Information).

The 100-kyr phase lag between δ^{18}O and eccentricity is calculated by cross-wavelet analysis using MATLAB codes written by Torrence, Compo and Grinsted[28]. Rayleigh's *R* (ref. 29) is defined as

$$R = \frac{1}{N}\left|\sum_{i=0}^{n}\cos\phi_n + i\sin\phi_n\right|$$

where ϕ_n is the phase lag of the *n*th 100-kyr window relative to eccentricity and the line brackets indicate the magnitude. *R* has a maximum value of 1.0 when all cycles have the same phase lag. This calculation is identical to that used previously[5,6], except that I anlayse 1.2 to 0 Myr ago and use cross-wavelet phase lags sampled every 100-kyr instead of the instantaneous phase of each termination. The significance of eccentricity pacing is also tested with the same Monte Carlo model used in refs 5 and 6. Ice volume is simulated as a random walk with an average 1-kyr step size of 1 and standard deviation of 2. When ice volume exceeds 90, it is stepped back to 0 over the next 10 kyr. The model's average cycle length is 100 kyr with a standard deviation of 20 kyr. The effects of age-model uncertainty and different noise parameterizations are presented in the Supplementary Information.

Time-dependent 100-kyr power, for example, in equation (1) and Fig. 3, is estimated by the squared fast Fourier transform of a moving 600-kyr boxcar filter using a frequency band of 0.0078–0.0110 kyr^{-1}. The parameter values for equation (1) are estimated by minimizing the mean square error between the logarithm of 100-kyr power in the model and data. I use the logarithm of power because the amount of 100-kyr power in δ^{18}O changes by two orders of magnitude from 5 to 0 Myr ago (Fig. 3a). Supplementary Table S2 compares results for a variety of optimization schemes.

Relating spectral estimates of time-dependent power to theoretical time-dependent spectra is statistically difficult[30], and the use of correlation coefficients to compare non-zero frequency intervals makes the false assumption that spectral power is derived from a random process. However, similar patterns of variability are observed using either windowed fast Fourier transform or wavelet analysis (Fig. 1), and several different spectral analysis techniques and parameterizations yield correlations of −0.69 to −0.59 for the 100-kyr power of eccentricity and δ^{18}O (Supplementary Table S1). It is beyond the scope of this study to quantify all sources of uncertainty in estimates of 100-kyr power, their correlations and estimated model parameters; therefore, the anticorrelation between the 100-kyr power of δ^{18}O and eccentricity should be considered a qualitative description intended to inspire future investigation.

Received 27 July 2009; accepted 1 March 2010; published online 4 April 2010

References

1. Hays, J. D., Imbrie, J. & Shackleton, N. J. Variations in the Earth's orbit: Pacemaker of the ice ages. *Science* **194,** 1121–1132 (1976).
2. Imbrie, J. *et al.* On the structure and origin of major glaciation cycles 2. The 100,000-year cycle. *Paleoceanography* **8,** 699–735 (1993).
3. Clemens, S. C. & Tiedemann, R. Eccentricity forcing of Pliocene-early Pleistocene climate revealed in a marine oxygen-isotope record. *Nature* **385,** 801–804 (1997).
4. Raymo, M. E. The timing of major terminations. *Paleoceanography* **12,** 577–585 (1997).
5. Huybers, P. & Wunsch, C. Obliquity pacing of the late Pleistocene glacial terminations. *Nature* **434,** 491–494 (2005).
6. Huybers, P. Glacial variability over the last two million years: An extended depth-derived agemodel, continuous obliquity pacing, and the Pleistocene progression. *Quat. Sci. Rev.* **26,** 37–55 (2007).
7. Liu, Z., Cleaveland, L. C. & Herbert, T. D. Early onset and origin of 100-kyr cycles in Pleistocene tropical SST records. *Earth Planet. Sci. Lett.* **265,** 703–715 (2008).
8. Saltzman, B., Hansen, A. & Maasch, K. The late Quaternary glaciations as the response of a three-component feedback system to Earth-orbital forcing. *J. Atmos. Sci.* **41,** 3380–3389 (1984).

9. Gildor, H. & Tziperman, E. Sea ice as the glacial cycles climate switch: Role of seasonal and orbital forcing. *Paleoceanography* **15,** 605–615 (2000).
10. Tziperman, E., Raymo, M. E., Huybers, P. C. & Wunsch, C. Consequences of pacing the Pleistocene 100 kyr ice ages by nonlinear phase locking to Milankovitch forcing. *Paleoceanography* **21,** PA4206 (2006).
11. Ridgwell, A. J., Watson, A. J. & Raymo, M. E. Is the spectral signature of the 100 kyr glacial cycle consistent with a Milankovitch origin? *Paleoceanography* **14,** 437–440 (1999).
12. Nie, J., King, J. & Fang, X. Late Pliocene–early Pleistocene 100-ka problem. *Geophys. Res. Lett.* **35,** L21606 (2008).
13. Parrenin, F. & Paillard, D. Amplitude and phase of glacial cycles from a conceptual model. *Earth Planet. Sci. Lett.* **214,** 243–250 (2003).
14. Shackleton, N. J. The 100,000-year ice-age cycle identified and found to lag temperature, carbon dioxide, and orbital eccentricity. *Science* **289,** 1897–1902 (2000).
15. Mudelsee, M. & Schulz, M. The mid-Pleistocene climate transition: Onset of 100 ka cycle lags ice volume build-up by 280 ka. *Earth Planet. Sci. Lett.* **151,** 117–123 (1997).
16. Lisiecki, L. E. & Raymo, M. E. A Pliocene–Pleistocene stack of 57 globally distributed benthic δ^{18}O records. *Paleoceanography* **20,** PA1003 (2005).
17. Clark, P. U. *et al.* The middle Pleistocene transition: Characteristics, mechanisms, and implications for long-term changes in atmospheric pCO_2. *Qaut. Sci. Rev.* **25,** 3150–3184 (2006).
18. Kawamura, K. *et al.* Northern Hemisphere forcing of climatic cycles in Antarctica over the past 360,000 years. *Nature* **448,** 912–917 (2007).
19. Paillard, D. The timing of Pleistocene glaciations from a simple multiple-state climate model. *Nature* **391,** 378–381 (1998).
20. Lisiecki, L. E. & Raymo, M. E. Plio-Pleistocene climate evolution: Trends and transitions in glacial cycle dynamics. *Quat. Sci. Rev.* **26,** 56–69 (2007).
21. Imbrie, J. & Imbrie, J. Z. Modelling the climatic response to orbital variations. *Science* **207,** 943–953 (1980).
22. Raymo, M. E., Lisiecki, L. E. & Nisancioglu, K. H. Plio-Pleistocene ice volume, Antarctic climate, and the global δ^{18}O record. *Science* **313,** 492–495 (2006).
23. Medina-Elizalde, M. & Lea, D. W. The mid-Pleistocene transition in the tropical Pacific. *Science* **310,** 1009–1012 (2005).
24. Saltzman, B. & Maasch, K. A. Carbon cycle instability as a cause of the Late Pleistocene ice age oscillations: Modeling the asymmetric response. *Glob. Biogeochem. Cycles* **2,** 177–185 (1988).
25. Toggweiler, J. R. Origin of the 100,000-year timescale in Antarctic temperatures and atmospheric CO_2. *Paleoceanography* **23,** PA2211 (2008).
26. Cande, S. C. & Kent, D. V. Revised calibration of the geomagnetic polarity timescale for the Late Cretaceous and Cenozoic. *J. Geophys. Res.* **100(B4),** 6093–6095 (1995).
27. Shackleton, N. J., Crowhurst, S., Hagelberg, T., Pisias, N. G. & Schneider, D. A. A new late Neogene time scale: Application to Leg 138 sites. *Proc. Ocean Drill. Program Sci. Results* **138,** 73–101 (1995).
28. Grinsted, A., Moore, J. C. & Jevrejeva, S. Application of the cross wavelet transform and wavelet coherence to geophysical time series. *Nonlinear Process. Geophys.* **11,** 561–566 (2004).
29. Upton, G. & Fingleton, B. *Spatial Data Analysis by Example* Vol. 2 (John Wiley, 1989).
30. Priestley, M. B. Wavelets and time-dependent spectral analysis. *J. Time Ser. Anal.* **17,** 85–103 (1996).

Acknowledgements

I thank T. Herbert, D. Lea and M. Raymo for many useful discussions.

Additional information

The author declares no competing financial interests. Supplementary information accompanies this paper on www.nature.com/naturegeoscience. Reprints and permissions information is available online at http://npg.nature.com/reprintsandpermissions.